

## Polymeric Films with Three Different Orientations of Crystalline-Phase Empty Channels

Alexandra R. Albunia,\* Paola Rizzo, and Gaetano Guerra

Dipartimento di Chimica and INSTM Research Unit, Università degli Studi di Salerno, Via Ponte don Melillo, 84084, Fisciano, Italy

Received April 7, 2009

The uniplanar orientations that can be achieved for the  $\epsilon$  phase of syndiotactic polystyrene, i.e., the first polymeric crystalline phase exhibiting channel-shaped porosity, have been explored by wide-angle X-ray diffraction. The formation of three different uniplanar orientations, presenting the three unit-cell axes perpendicular to the film plane, can be controlled by suitable processes, which are based on combined solvent-induced crystallizations and on thermal treatments. This allows gaining control of three different orientations of the crystalline nanochannels with respect to the film surface and hence control of diffusivity as well as orientation of low-molecular-mass guest molecules, also at the macroscopic scale.

### Introduction

Materials exhibiting one-dimensional channels are very attractive hosts for active guest molecules. Channel with diameters in the range 5–200 nm have been obtained by several different nanotechnologies.<sup>1</sup> On the other hand, channel with diameters smaller than 1–2 nm have been obtained only by spontaneous organization of nanoporous crystalline phases, mostly zeolites.<sup>2</sup> It is worth adding that the crystalline nature of these nanoporous materials allows for obtaining the orientation of the channels for whole crystals, which can reach micrometric sizes.<sup>2</sup>

Recently, a polymeric nanoporous crystalline phase exhibiting channels parallel to the chain axes has been discovered for a commercial and robust stereoregular

polymer (syndiotactic polystyrene, s-PS).<sup>3</sup> This is the orthorhombic  $\epsilon$  phase,<sup>4</sup> with  $a = 1.61$  nm,  $b = 2.18$  nm, and  $c = 0.79$  nm and four chains per unit cell, which presents a minimum center-to-center distance between channels of 1.36 nm and a density close to 0.98 g/cm<sup>3</sup>, i.e., definitely lower than the density of the corresponding amorphous phase (1.05 g/cm<sup>3</sup>). The density is similar to that one of the  $\delta$  phase,<sup>5</sup> a well-known nanoporous crystalline phase of s-PS (monoclinic with  $a = 1.74$  nm,  $b = 1.185$  nm,  $c = 0.77$  nm, and  $\gamma = 117^\circ$ , with two chains per

\*Corresponding author. Tel.: 39 (0) 89 969392. Fax: 39 (0) 89 969603. E-mail: aalbunia@unisa.it.

- (1) (a) Yao, B.; Fleming, D.; Morris, M.A.; Lawrence, S.E. *Chem. Mater.* **2004**, *16*, 4851–4855. (b) Yamaguchi, A.; Uejo, F.; Yoda, T.; Uchida, T.; Tanamura, Y.; Yamashita, T.; Teramae, N. *Nat. Mater.* **2004**, *3*, 337. (c) Mamontov, E.; Kumzerov, Yu.A.; Vakhshushev, *Phys. Rev. E* **2005**, *72*, 051502. (d) Platschek, B.; Petkov, N.; Bein, T. *Angew. Chem., Int. Ed.* **2006**, *45*, 1134–1138. (e) Yu, Y.; Qiu, H.; Wu, X.; Li, H.; Li, Y.; Sakamoto, Y.; Inoue, Y.; Sakamoto, K.; Terasaki, O.; Che, S. *Adv. Funct. Mater.* **2008**, *18*, 541–550. (f) Nikoobakht, B. *Chem. Mater.* **2009**, *21*, 27–32.
- (2) (a) Uryadov, A. V.; Skirda, V. D. *Magn. Reson. Imaging* **2001**, *19*, 429–32. (b) Ganschow, M.; Hellriegel, C.; Kneuper, E.; Wark, M.; Thiel, C.; Schulz-Ekloff, G.; Braeuchle, C.; Woehle, D. *Adv. Funct. Mater.* **2004**, *14*, 269–276. (c) Ruiz, A.Z.; Li, H.; Calzaferri, G. *Angew. Chem., Int. Ed.* **2006**, *45*, 5282–5287. (d) Zhai, J. P.; Lee, H. F.; Li, I. L.; Ruan, S. C.; Tang, Z. K. *Nanotechnology* **2008**, *19*, 175604/1–175604/5. (e) Choi, J.M.; Jeong, S.H.; Hwang, D.K.; Im, S.; Lee, B.H.; Sung, M.M. *Org. Electron.* **2009**, *10*, 199–204.
- (3) (a) Guerra, G.; Vitagliano, M.V.; De Rosa, C.; Petraccone, V.; Corradini, P. *Macromolecules* **1990**, *23*, 1539. (b) Malanga, M. *Adv. Mater.* **2000**, *12*, 1869. (c) Schellenberg, J.; Tomotsu, N. *Prog. Polym. Sci.* **2002**, *27*, 1925. (d) Milano, G.; Guerra, G. *Progr. Mater. Sci.* **2009**, *54*, 68.
- (4) (a) Rizzo, P.; Daniel, C.; De Girolamo Del Mauro, A.; Guerra, G. *Chem. Mater.* **2007**, *19*, 3864. (b) Rizzo, P.; D'Aniello, C.; De Girolamo Del Mauro, A.; Guerra, G. *Macromolecules* **2007**, *40*, 9470. (c) Petraccone, V.; Ruiz, O.; Tarallo, O.; Rizzo, P.; Guerra, G. *Chem. Mater.* **2008**, *20*, 3663.
- (5) (a) De Rosa, C.; Guerra, G.; Petraccone, V.; Pirozzi, B. *Macromolecules* **1997**, *30*, 4147. (b) Milano, G.; Venditto, V.; Guerra, G.; Cavallo, L.; Ciambelli, P.; Sannino, D. *Chem. Mater.* **2001**, *13*, 1506. (c) Gowd, E. B.; Shibayama, N.; Tashiro, K. *Macromolecules* **2006**, *39*, 8412.
- (6) (a) Manfredi, C.; Del Nobile, M. A.; Mensitieri, G.; Guerra, G.; Rapacciuolo, M. *J. Polym. Sci., Polym. Phys. Ed.* **1997**, *35*, 133. (b) Guerra, G.; Manfredi, C.; Musto, P.; Tavone, S. *Macromolecules* **1998**, *31*, 1329. (c) Musto, P.; Manzari, M.; Guerra, G. *Macromolecules* **2000**, *33*, 143. (d) Musto, P.; Mensitieri, G.; Cotugno, S.; Guerra, G.; Venditto, V. *Macromolecules* **2002**, *35*, 2296. (e) Larobina, D.; Sanguigno, L.; Venditto, V.; Guerra, G.; Mensitieri, G. *Polymer* **2004**, *45*, 429. (f) Mahesh, K.P.O.; Sivakumar, M.; Yamamoto, Y.; Tsujita, Y.; Yoshimizu, H.; Okamoto, S. *J. Membr. Sci.* **2005**, *262*, 11. (g) Sivakumar, M.; Mahesh, K. P. O.; Yamamoto, Y.; Yoshimizu, H.; Tsujita, Y. *J. Polym. Sci., Polym. Phys.* **2005**, *43*, 1873. (h) Daniel, C.; Alfano, D.; Venditto, V.; Cardea, S.; Reverchon, E.; Larobina, D.; Mensitieri, G.; Guerra, G. *Adv. Mater.* **2005**, *17*, 1515. (i) Malik, S.; Roizard, D.; Guenet, J.M. *Macromolecules* **2006**, *39*, 5957. (j) Mensitieri, G.; Larobina, D.; Guerra, G.; Venditto, V.; Femeglia, M.; Priol, S. *J. Polym. Sci., Part B: Polym. Phys.* **2008**, *46*, 8. (k) Daniel, C.; Sannino, D.; Guerra, G. *Chem. Mater.* **2008**, *20*, 577.
- (7) (a) Mensitieri, G.; Venditto, V.; Guerra, G. *Sens. Actuators, B* **2003**, *92*, 255. (b) Giordano, M.; Russo, M.; Cusano, A.; Cutolo, A.; Mensitieri, G.; Nicolais, L. *Appl. Phys. Lett.* **2004**, *85*, 92. (c) Cusano, A.; Pilla, P.; Contessa, L.; Iadicicco, A.; Campopiano, S.; Cutolo, A.; Giordano, M.; Guerra, G. *Appl. Phys. Lett.* **2005**, *87*, 234105. (d) Giordano, M.; Russo, M.; Cusano, A.; Mensitieri, G.; Guerra, G. *Sens. Actuators, B* **2005**, *109*, 177. (e) Cusano, A.; Iadicicco, A.; Pilla, P.; Contessa, L.; Campopiano, S.; Cutolo, A.; Giordano, M.; Guerra, G. *J. Lightwave Technol.* **2006**, *24*, 1776. (f) Buono, A.; Rizzo, P.; Immediata, I.; Guerra, G. *J. Am. Chem. Soc.* **2007**, *129*, 10992. (g) Guadagno, L.; Raimondo, M.; Silvestre, C.; Immediata, I.; Rizzo, P.; Guerra, G. *J. Mater. Chem.* **2008**, *18*, 567.

unit cell), which presents the empty space distributed as isolated cavities rather than as channels. Several literature reports have shown that materials presenting these nanoporous s-PS phases are promising for applications in chemical separations<sup>6</sup> (mainly air/water purification) as well as in sensorics.<sup>7</sup>

Polymer crystals, although generally much smaller than inorganic and organic crystals, present the advantage of easy orientation, also at the macroscopic scale. In fact, for all semicrystalline polymers, it is easy to get axial orientation of the crystalline phases, by imposing the alignment of the polymer chain axes (generally assumed coincident with the crystallographic  $c$  axis) parallel to a stretching direction. Moreover, as for s-PS films exhibiting co-crystalline phases with low-molecular-mass molecules,<sup>8</sup> it is possible to achieve the unprecedented formation of three different kinds<sup>9</sup> of uniplanar orientations.<sup>10</sup>

The three uniplanar orientations of s-PS co-crystalline films correspond to the three simplest orientations of the high planar-density  $ac$  layers (i.e., layers of close-packed alternated enantiomorphous s-PS helices that characterize most s-PS co-crystalline phases as well as the nanoporous  $\delta$  phase) with respect to the film plane. As shown by the scheme 1 these three uniplanar orientations have been named  $a_{//} c_{//}$ ,  $a_{//} c_{\perp}$ , and  $a_{\perp} c_{//}$ , indicating crystalline phase orientations presenting the  $a$  and  $c$  (chain) axes parallel ( $//$ ) or perpendicular ( $\perp$ ) to the film plane.<sup>9g</sup> The degree and the kind of uniplanar orientation depends on the selected technique (solution crystallizations or solvent induced crystallizations or recrystallizations) as well as on the chemical nature of the guest.<sup>9</sup> The three uniplanar orientations that can be achieved for s-PS co-crystalline phases can be maintained (without substantial loss of their degree of orientation) after guest extraction procedures leading to the  $\delta$  phase, as well as after thermal annealing procedures<sup>9a,9d</sup> leading to the dense helical  $\gamma$  phase,<sup>11</sup> which

is also the most suitable precursor phase for the preparation of the channeled  $\varepsilon$  phase.<sup>4</sup> It is also worth adding that some orientational order can be maintained after crystal-to-crystal transitions involving chain conformational changes from the helical to the zig-zag planar. In fact, suitable thermal treatments on s-PS films presenting the three different uniplanar orientations of their helical crystalline phases can lead to films with planar orientations of their zig-zag planar  $\alpha^{12}$  and  $\beta^{13}$  crystalline phases, where only the perpendicular ( $c_{\perp}$ ) or parallel ( $c_{//}$ ) chain axes orientation is maintained.<sup>9a</sup>

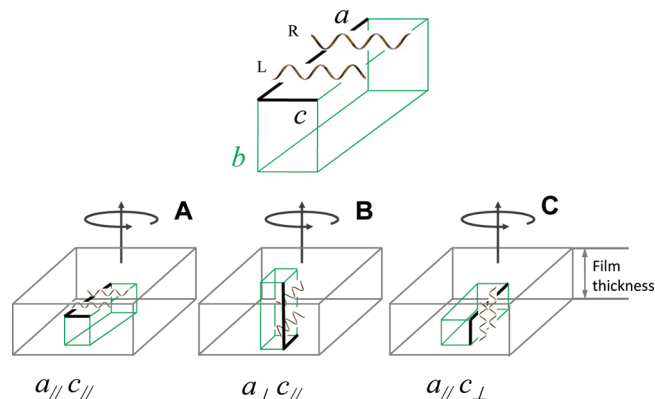
The availability of s-PS films with three different kinds of uniplanar orientation allows us to establish fine structural features, e.g., experimental evaluation of the orientation of transition moment vectors of host and guest vibrational modes.<sup>14</sup> It also allows active guest orientation control<sup>15</sup> for co-crystalline advanced materials (fluorescent, photoreactive, nonlinear optical, magnetic).<sup>16</sup> Moreover, for the  $\delta$  nanoporous phase, the three different kinds of uniplanar orientation have been shown to be helpful to control guest diffusivity.<sup>17</sup>

As for the recently discovered nanoporous  $\varepsilon$  phase, the information available relative to the possible occurrence of some kind of uniplanar orientation is scarce. In particular, it has been reported that by chloroform-induced recrystallization on unoriented  $\gamma$ -form films, followed by chloroform extraction,  $\varepsilon$ -form films are obtained that exhibit an orientation of chain axes of their crystalline phase being preferentially perpendicular to the film surface ( $f_{002} \approx 0.7$ ).<sup>9f</sup>

In this paper, the kind and degree of uniplanar orientations that can be achieved for the nanoporous  $\varepsilon$  phase, as obtained from  $\gamma$ -form films, exhibiting high degrees of uniplanar  $a_{//} c_{//}$ ,  $a_{\perp} c_{//}$ , and  $a_{//} c_{\perp}$  orientations, have been

- (8) (a) Chatani, Y.; Inagaki, T.; Shimane, Y.; Ijitsu, T.; Yukimori, T.; Shikuma, H. *Polymer* **1993**, *34*, 1620. (b) Chatani, Y.; Shimane, Y.; Inagaki, T.; Shikuma, H. *Polymer* **1993**, *34*, 4841. (c) De Rosa, C.; Rizzo, P.; Ruiz, O.; Petraccone, V.; Guerra, G. *Polymer* **1999**, *40*, 2103. (d) Tarallo, O.; Petraccone, V. *Macromol. Chem. Phys.* **2004**, *205*, 1351. (e) Tarallo, O.; Petraccone, V. *Macromol. Chem. Phys.* **2005**, *206*, 672. (f) Petraccone, V.; Tarallo, O.; Venditto, V.; Guerra, G. *Macromolecules* **2005**, *38*, 6965. (g) Tarallo, O.; Petraccone, V.; Venditto, V.; Guerra, G. *Polymer* **2006**, *47*, 2402. (h) Tarallo, O.; Petraccone, V.; Daniel, C.; Guerra, G. *Cryst. Eng. Commun.* **2009**, submitted.
- (9) (a) Rizzo, P.; Lamberti, M.; Albulia, A. R.; Ruiz, O.; Guerra, G. *Macromolecules* **2002**, *35*, 5854. (b) Rizzo, P.; Costabile, A.; Guerra, G. *Macromolecules* **2004**, *37*, 3071. (c) Rizzo, P.; Della Guardia, S.; Guerra, G. *Macromolecules* **2004**, *37*, 8043. (d) Rizzo, P.; Spatola, A.; De Girolamo Del Mauro, A.; Guerra, G. *Macromolecules* **2005**, *38*, 10089. (e) Daniel, C.; Avallone, A.; Rizzo, P.; Guerra, G. *Macromolecules* **2006**, *39*, 4820. (f) Albulia, A. R.; Annunziata, L.; Guerra, G. *Macromolecules* **2008**, *41*, 2683. (g) Albulia, A. R.; Rizzo, P.; Tarallo, O.; Petraccone, V.; Guerra, G. *Macromolecules* **2008**, *41*, 8632–8642.
- (10) (a) Heffelfinger, C. J.; Burton, R. L. *J. Polym. Sci.* **1960**, *47*, 289. (b) Werner, E.; Janocha, S.; Hopper, M. J. *Mackenzie Encyclopedia of Polymer Science and Engineering*, 2nd ed.; Wiley-Interscience: New York, 1986; Vol. 12, p 193. (c) Gohil, R. M. *J. Appl. Polym. Sci.* **1993**, *48*, 1649. (d) Rizzo, P.; Venditto, V.; Guerra, G.; Vecchione, A. *Macromol. Symp.* **2002**, *185*, 53.
- (11) (a) Immirzi, A.; de Candia, F.; Iannelli, P.; Zambelli, A.; Vittoria, V. *Makromol. Chem., Rapid Commun.* **1988**, *9*, 761. (b) Tamai, Y.; Fukuda, M. *Macromol. Rapid Commun.* **2002**, *23*, 892. (c) Rizzo, P.; Albulia, A. R.; Guerra, G. *Polymer* **2005**, *46*, 9549.
- (12) (a) De Rosa, C.; Guerra, G.; Petraccone, V.; Corradini, P. *Polym. J.* **1991**, *23*, 1435. (b) Cartier, L.; Okihara, T.; Lotz, B. *Macromolecules* **1998**, *31*, 3303.
- (13) (a) De Rosa, C.; Rapacciuolo, M.; Guerra, G.; Petraccone, V.; Corradini, P. *Polymer* **1992**, *33*, 1423. (b) Chatani, Y.; Shimane, Y.; Ijitsu, T.; Yukinari, T. *Polymer* **1993**, *34*, 1625.
- (14) (a) Albulia, A. R.; Rizzo, P.; Guerra, G.; Torres, F. J.; Civalieri, B.; Zicovich-Wilson, C. M. *Macromolecules* **2007**, *40*, 3895. (b) Torres, F. J.; Civalieri, B.; Meyer, A.; Musto, P.; Albulia, A. R.; Rizzo, P.; Guerra, G. *J. Phys. Chem. B* **2009**, *113*, 5059.
- (15) (a) Albulia, A. R.; Di Masi, S.; Rizzo, P.; Milano, G.; Musto, P.; Guerra, G. *Macromolecules* **2003**, *36*, 8695. (b) Albulia, A. R.; Milano, G.; Venditto, V.; Guerra, G. *J. Am. Chem. Soc.* **2005**, *127*, 13114. (c) Itagaki, H.; Sago, T.; Uematsu, M.; Yoshioka, G.; Correa, A.; Venditto, V.; Guerra, G. *Macromolecules* **2008**, *41*, 9156–9164.
- (16) (a) Venditto, V.; Milano, G.; De Girolamo Del Mauro, A.; Guerra, G.; Mochizuki, J.; Itagaki, H. *Macromolecules* **2005**, *38*, 3696. (b) Stegmaier, P.; De Girolamo Del Mauro, A.; Venditto, V.; Guerra, G. *Adv. Mater.* **2005**, *17*, 1166. (c) Uda, Y.; Kaneko, F.; Tanigaki, N.; Kawaguchi, T. *Adv. Mater.* **2005**, *17*, 1846. (d) Kaneko, F.; Uda, Y.; Kajiwar, A.; Tanigaki, N. *Macromol. Rapid Commun.* **2006**, *27*, 1643. (e) D'Aniello, C.; Musto, P.; Venditto, V.; Guerra, G. *J. Mater. Chem.* **2007**, *17*, 531. (f) Daniel, C.; Galdi, N.; Montefusco, T.; Guerra, G. *Chem. Mater.* **2007**, *19*, 3302. (g) De Girolamo Del Mauro, A.; Carotenuto, M.; Venditto, V.; Petraccone, V.; Scoponi, M.; Guerra, G. *Chem. Mater.* **2007**, *19*, 6041.
- (17) (a) Milano, G.; Guerra, G.; Müller-Plathe, F. *Chem. Mater.* **2002**, *14*, 2977. (b) Venditto, V.; De Girolamo Del Mauro, A.; Mensitieri, G.; Milano, G.; Musto, P.; Rizzo, P.; Guerra, G. *Chem. Mater.* **2006**, *18*, 2205. (c) Annunziata, L.; Albulia, A. R.; Venditto, V.; Guerra, G. *Macromolecules* **2006**, *39*, 9166. (d) Albulia, A. R.; Minucci, T.; Guerra, G. *J. Mater. Chem.* **2008**, *18*, 1046.

**Scheme 1. Schematic Presentation of the Three Uniplanar Orientations of s-PS Cocrystalline Films, Corresponding to the Three Simplest Orientations of the High-Planar-Density  $ac$  Layers with Respect to the Film Plane**



explored by wide-angle X-ray diffraction analysis. The paper shows that three different uniplanar orientations can be achieved also for the  $\epsilon$  phase, thus getting three different orientations of the crystalline nanochannels with respect to the surface of also macroscopic films.

### Results And Discussion

X-ray diffraction patterns of the  $\epsilon$ -form s-PS films, as obtained by recrystallization by chloroform vapor sorption followed by chloroform desorption by sample immersion in acetonitrile, on the  $\gamma$ -form films exhibiting  $a_{//} c_{//}$ ,  $a_{\perp} c_{//}$ , and  $a_{//} c_{\perp}$  uniplanar orientations (whose X-ray diffraction patterns are shown in Figure S1A–C in the Supporting Information) are shown in Figure 1A–C, respectively. In particular, the EDGE patterns, i.e., photographic patterns taken with X-ray beam parallel to the film surface, are shown as Figures 1A–C, whereas the THROUGH patterns, i.e., photographic patterns taken with X-ray beam perpendicular to the film surface (which present uniform Debye rings and for the sake of clarity are shown as diffraction intensity profiles), are shown as Figure 1A'–C', respectively.

For an easier reading of the EDGE patterns, the diffraction intensity profiles, as collected along the horizontal lines indicating the direction normal to the film plane, are shown in Figure 2A''–C''. For the sake of comparison, analogous diffraction profiles are reported for the precursor  $\delta$ - and  $\gamma$ -form films in Figure 2 A–C and A'–C', respectively.

Particularly simple is the interpretation of the results relative to the films with  $a_{//} c_{\perp}$  uniplanar orientation (Figures 1C and 2C). In fact, it is immediately apparent that, as for the  $\delta$  (Figure 2C) and  $\gamma$  phase (Figure 2C') precursors, the corresponding  $\epsilon$  phase film (Figures 1C and 2C'') present an intense 002 reflection at  $2\theta_{\text{CuK}\alpha} \approx 22.5^\circ$ , corresponding to  $c$  axis periodicity of 0.79 nm. A quantitative evaluation of the orientation function ( $f_{002} \approx 0.85$ ) clearly indicates the complete maintenance of the orientation of the crystalline phase chain axes, preferentially perpendicular to the film plane, being present in the precursor  $\delta$  and  $\gamma$  films.

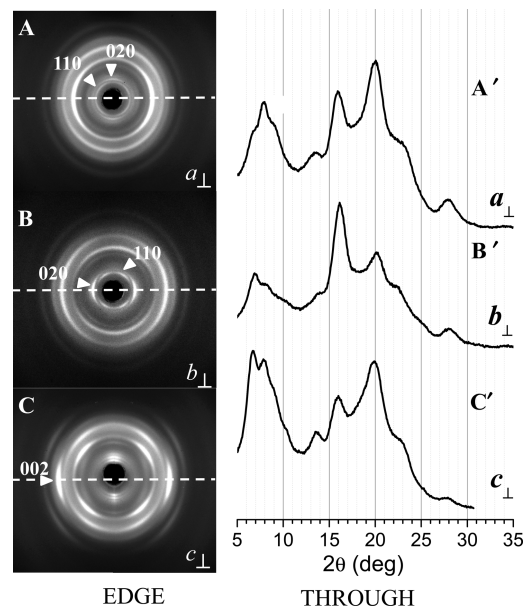


**Figure 1.** X-ray diffraction patterns of three s-PS films, presenting different kinds of uniplanar orientation of the nanoporous crystalline phase. (A–C) Photographic patterns taken with X-ray beam parallel to the film surface (EDGE patterns). (A'–C') Diffraction profiles of photographic patterns taken with X-ray beam perpendicular to the film surface (THROUGH patterns). The three orientations can be defined as  $a_{\perp}$ ,  $b_{\perp}$ , and  $c_{\perp}$ , respectively, thus indicating that the three unit-cell axes are preferentially perpendicular to the film surface. Dashed horizontal lines indicate the direction normal to the film plane.

The EDGE diffraction patterns of the  $\epsilon$ -form films (Figures 1B and 2B''), as derived from  $\delta$ - (Figure 2B) and  $\gamma$ -form (Figure 2B') films with  $a_{\perp} c_{//}$  uniplanar orientation, show on the horizontal line an intense 020 reflection typical of the  $\epsilon$  phase (corresponding to a Bragg distances  $d = 1.08$  nm, i.e., at  $2\theta_{\text{CuK}\alpha} \approx 8.2^\circ$ ). This clearly suggests that the  $\delta$ - and  $\gamma$ -form films with their  $a$  axis perpendicular to the film plane and their  $c$  axes parallel to the film plane are transformed, by the used re-crystallization procedure, into  $\epsilon$ -form films with their  $a$  and  $c$  axes both preferentially parallel to the film plane. This has been confirmed by a quantitative comparison between observed and calculated azimuthal angles associated with  $\epsilon$ -form reflections (shown in Table S2 of the Supporting Information and prepared by using a procedure analogous to that one used for the  $\delta$  phase to prepare Table 1 of ref 9g).

The observed transformation, because the  $\epsilon$  phase is orthorhombic, produces an orientation of its  $b$  axis preferentially perpendicular to the film surface, which can be formally indicated as

$$a(\delta)_{\perp} c_{//} \rightarrow a(\gamma)_{\perp} c_{//} \rightarrow b(\epsilon)_{\perp}$$

Quantitative evaluations indicate some reduction of the degree of orientation, which for the precursor  $\gamma$ -form film (Figure S1B in the Supporting Information) is  $f_{020} \approx -0.43$ , whereas that for the  $\epsilon$ -form film of Figure 1B is  $f_{020} \approx 0.74$  (rather than 0.86, as would be expected for a complete maintenance of uniplanar orientation).

The EDGE diffraction patterns of the  $\epsilon$ -form films (Figures 1A and 2A''), as derived from  $\delta$ - (Figure 2A)



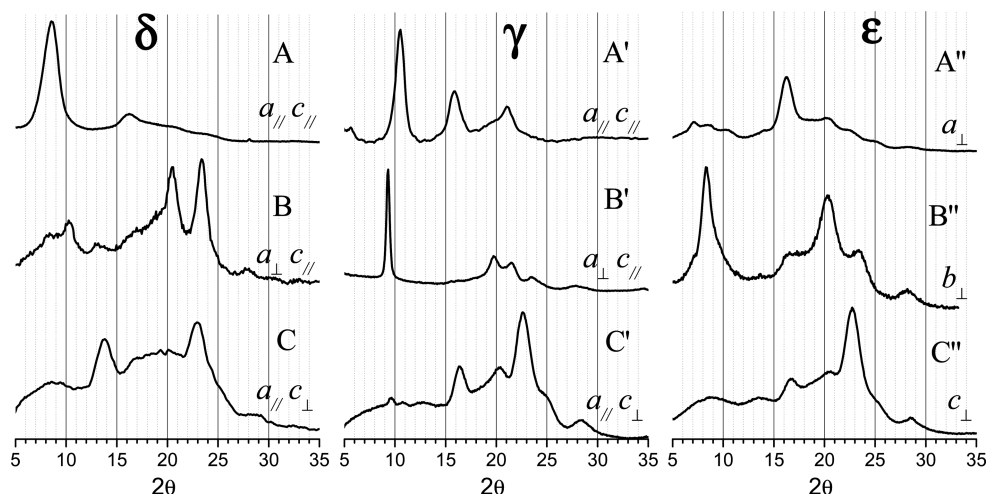


**Figure 2.** Diffraction profiles of photographic patterns taken with X-ray beam parallel to the film surface (EDGE patterns) of s-PS films, presenting different kinds of uniplanar orientation of the crystalline phases:  $\delta$  (A–C),  $\gamma$  (A'–C'), and  $\epsilon$  (A''–C''), respectively.

**Table 1.** Diffusivities (expressed as  $\text{cm}^2/\text{s}$ ) of Ethylene in  $\delta$  and  $\epsilon$  Films of s-PS, Exhibiting the Three Different Uniplanar Orientations As Schematically Shown in Figure 3

$\delta$		$\epsilon$	
$a_{  }c_{  }$ ( $f_{0k0} \approx 0.81$ )	$1.7 \times 10^{-10}$	$a_{\perp}$ ( $f_{0k0} \approx -0.37$ )	$11 \times 10^{-10}$
$a_{\perp}c_{  }$ ( $f_{0k0} \approx -0.43$ )	$9.3 \times 10^{-10}$	$b_{\perp}$ ( $f_{0k0} \approx 0.74$ )	$6.8 \times 10^{-10}$
$a_{  }c_{\perp}$ ( $f_{00l} \approx 0.85$ )	$1.5 \times 10^{-10}$	$c_{\perp}$ ( $f_{00l} \approx 0.85$ )	$13 \times 10^{-10}$

and  $\gamma$ -form (Figure 2A') films with  $a_{||} c_{||}$  uniplanar orientation, show that no  $\epsilon$ -form reflection is centered on the horizontal line. On the other hand, the 020 reflection is centered on the vertical line, clearly suggesting that the  $\delta$ - and  $\gamma$ -form films with their  $a$  and  $c$  axes parallel to the film plane are transformed, by the used recrystallization procedure, into  $\epsilon$ -form films with their  $a$  axis preferentially perpendicular to the film plane and  $c$  axes preferentially parallel to the film plane.

The observed transformation between different uniplanar orientations, can be formally indicated as

$$a(\delta)_{||} c_{||} \rightarrow a(\gamma)_{||} c_{||} \rightarrow a(\epsilon)_{\perp}$$

Also in this case, quantitative evaluations indicate some reduction of the degree of orientation, which for the precursor  $\gamma$ -form film (Figure S1A in the Supporting Information) is  $f_{020} \approx 0.81$ , whereas that for the  $\epsilon$ -form film of Figure 1A is  $f_{020} \approx -0.37$  (rather than  $-0.405$ , as would be expected for a complete maintenance of uniplanar orientation).

Schematic presentations of the three different uniplanar orientations that have been achieved for the nanoporous  $\epsilon$  phase (D–F), as well as the corresponding three uniplanar orientations of the precursor  $\delta$  phase (A–C), are shown in Figure 3. For the sake of clarity, the trace of the film surface and direction of the film thickness are clearly indicated. The  $\epsilon$ -form film with ideal  $c_{\perp}$  uniplanar orientation (Figure 3F) presents its empty channels perpendicular to the film surface while films with ideal  $b_{\perp}$  and  $a_{\perp}$  uniplanar orientations (panels D and E in Figure 3) present their empty channels parallel to the film surface.

The along-the-chain view of the molecular models (panels D and E in Figure 3) of the  $\epsilon$  phase also suggest

that the direction of preferential interchannel guest diffusivity is the  $a$  axis (also pointed out by a red dotted line). This direction is perpendicular to the film surface for the  $a_{\perp}$  orientation (Figure 3D), whereas it is parallel to the film surface for the  $b_{\perp}$  orientation (Figure 3E). These simple geometrical considerations allow us to anticipate that for  $\epsilon$ -form films, the uniplanar orientations that are expected to maximize and minimize guest diffusivity in the direction perpendicular to the film surface are  $c_{\perp}$  and  $b_{\perp}$ , respectively.

This prediction is confirmed by a comparison between ethylene desorption kinetics from  $\epsilon$ -form films and from the precursor  $\delta$ -form films, as obtained from the absorbance variations of the ethylene infrared absorption peak at  $952 \text{ cm}^{-1}$ <sup>17d</sup> (Fick's plots in Figure 4 and corresponding diffusivity data in Table 1). In fact, for the  $\delta$ -form films (as already known for several guests: 1,2-dichloroethane,<sup>17b</sup> carbon dioxide,<sup>17c</sup> or ethylene<sup>17d</sup> and in agreement with molecular modeling predictions)<sup>17a</sup> the maximum diffusivity (Figure 4A and Table 1) is observed for the orientation presenting the  $a$  axis perpendicular to the film surface ( $a_{\perp}c_{||}$ , Figure 3B). On the other hand, for the  $\epsilon$ -form film with  $b_{\perp}$  orientation (Figure 3E), which is obtained by the  $\delta$ -form precursor, presenting the  $a$  axis perpendicular to the film surface ( $a_{\perp}c_{||}$ ), a minimum of ethylene diffusivity is instead observed.

It is worth adding that for films presenting similar crystallinity and similar degree of perpendicular orientation of the  $c$  (chain) axes (third row in Table 1), the  $\epsilon$  phase, exhibiting a channel-shaped nanoporosity, presents an increase in ethylene diffusivity of nearly one order of magnitude with respect to the  $\delta$  phase, exhibiting a cavity-shaped nanoporosity.

X-ray diffraction studies, analogous to those reported in Figure 1, have shown that not only the kind but also the degree of uniplanar orientation of the nanoporous  $\epsilon$  crystalline phase can be fully retained after sorption into the nanochannels of suitable low-molecular-mass guest molecules (e.g., 1,2-dichloroethane<sup>4c</sup> or 4-nitro-aniline<sup>4a</sup>), leading to the formation of co-crystalline phases that can be named  $\epsilon$ -clathrates.

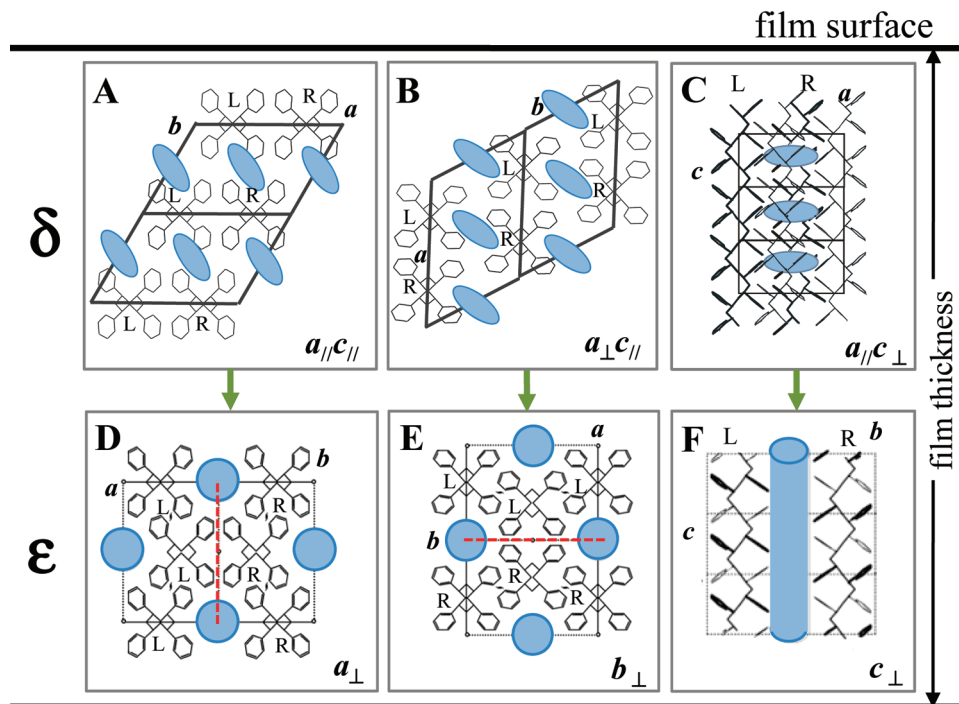


**Figure 3.** Representation of the limit ordered uniplanar orientations for the nanoporous  $\delta$  (A–C) and  $\epsilon$  (D–F) crystalline phases. The symbols  $\perp$  and  $\parallel$  indicate crystal axes being perpendicular and parallel to the film surface, respectively. Suitable procedures allow the transformation from the  $\delta$  orientations sketched in A–C into the  $\epsilon$  orientations sketched in D–F, respectively. The red lines indicate the possible preferential direction of interchannel guest diffusion for the  $\epsilon$  phase.

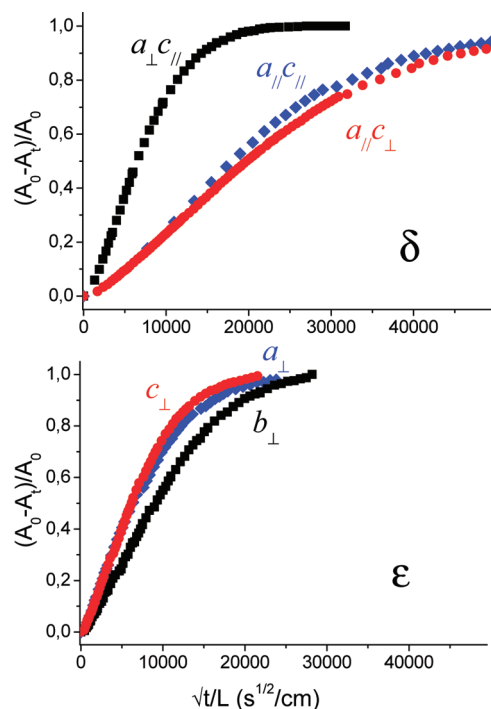


**Figure 4.** Ethylene desorption isotherms, presenting the absorbance variations of the  $952\text{ cm}^{-1}$  ethylene peak  $(A_0 - A_t)/A_0$  versus the square root of desorption time divided by film thickness ( $\sqrt{t}/L$ ), from polymeric films after equilibrium absorption at room temperature and at a pressure of 1 atm.  $\delta$ -Form or  $\epsilon$ -form s-PS films exhibit three different uniplanar orientations.  $\delta$ :  $a_{\parallel}c_{\parallel}$  ( $f_{010} \approx 0.81$ );  $a_{\perp}c_{\parallel}$  ( $f_{010} \approx -0.43$ );  $a_{\parallel}c_{\perp}$  ( $f_{002} \approx 0.85$ ).  $\epsilon$ :  $a_{\perp}$  ( $f_{020} \approx -0.37$ );  $b_{\perp}$  ( $f_{020} \approx 0.74$ );  $c_{\perp}$  ( $f_{002} \approx 0.85$ ). The corresponding limit ordered uniplanar orientations are sketched in Figure 3A–F, respectively. For the  $\epsilon$ -form films, the colors of the curves have been selected like those of the precursor  $\delta$ -form films.

Because of the low mobility of most guest molecules of  $\epsilon$ -clathrates,<sup>4a</sup> the control of the orientation of the channels of host  $\epsilon$  phase also allows the control of the

orientation of the enclosed guest molecules.<sup>4a</sup> As already observed for the co-crystalline phases based on the nanoporous  $\delta$  phase ( $\delta$ -clathrates and intercalates),<sup>8</sup> this orientation control could be particularly relevant for the case of active guests with functional properties.<sup>16</sup>

## Conclusions

Three different uniplanar orientations have been achieved for the nanoporous  $\epsilon$  phase of s-PS, corresponding to the  $a$ ,  $b$ , and  $c$  crystal axes preferentially perpendicular to the film surface. These three uniplanar orientations allow getting three different orientations of the crystalline nanochannels, typical of the  $\epsilon$  phase, with respect to the film surface and hence allow controlling the diffusivity of the guest molecules as well as the orientation of active guest molecules, also at the macroscopic scale. Molecular modeling studies, mainly based on guest molecular dynamics, analogous to those reported some years ago for the nanoporous  $\delta$  phase,<sup>17a</sup> are in progress for the nanoporous  $\epsilon$  phase.

## Experimental Section

**Materials and Preparation Procedures.** The s-PS was manufactured by Dow Chemical Company under the trademark Questra 101. The  $^{13}\text{C}$  nuclear magnetic resonance characterization showed that the content of syndiotactic triads was over 98%. The weight-average molar mass obtained by gel permeation chromatography (GPC) in trichlorobenzene at  $135\text{ }^{\circ}\text{C}$  was found to be  $M_w = 3.2 \times 10^5$  with the polydispersity index,  $M_w/M_n = 3.9$ . Pure solvents were purchased from Aldrich and used without further purification.

$\delta$ -Form films with the  $a_{\parallel}c_{\parallel}$  uniplanar orientation, having a thickness of  $25\text{--}40\text{ }\mu\text{m}$ , were obtained by casting procedure from 1% w/w solution in chloroform at room temperature.

$\delta$ -Form films with the  $a_{\perp} c_{\parallel}$  and  $a_{\parallel} c_{\perp}$  films, having a thickness of 100–150  $\mu\text{m}$ , were obtained by annealing amorphous s-PS films at 200 °C for 1 h (thus obtaining the  $\alpha$  crystalline phase) followed by immersion in suitable solvents for 1 day at room temperature and successive guest removal. In particular, films with the  $a_{\parallel} c_{\perp}$  uniplanar orientation were obtained by immersion in pure trichloroethylene,<sup>9f</sup> whereas films with the  $a_{\perp} c_{\parallel}$  uniplanar orientation were obtained by immersion in pure chloroform.<sup>9f</sup> The guest removal was obtained by extraction with carbon dioxide in supercritical conditions.<sup>18</sup> The residual guest content in the samples, after these extraction procedures, as evaluated by thermogravimetric measurements, was lower than 0.1%. The amorphous s-PS films were obtained by melt extrusion with an extrusion head of 200 mm  $\times$  0.5 mm.

$\gamma$ -Form films with uniplanar orientations were obtained by annealing of the corresponding nanoporous  $\delta$ -form films at 160 °C for 2 h. All the considered samples are semicrystalline with degree of crystallinity in the range 30–45%, as determined by the Fourier transform infrared method described in ref 19.

$\varepsilon$ -Form films with uniplanar orientations were obtained by recrystallization by chloroform vapor sorption followed by chloroform desorption by sample immersion in acetonitrile, on the oriented  $\gamma$ -form films, in turn obtained by annealing of the corresponding nanoporous  $\delta$ -form films at 130 °C for 1 h.

**Characterization Techniques.** Wide-angle X-ray diffraction patterns with nickel filtered CuK $\alpha$  radiation were obtained, in transmission, by using a cylindrical camera (radius = 57.3 mm). The patterns were recorded on a BAS-MS imaging plate (FUJIFILM) and processed with a digital imaging reader (FUJIBAS 1800). In particular, to recognize the kind of crystalline phase orientation, photographic X-ray diffraction patterns were taken by having the X-ray beam parallel (EDGE) and perpendicular (THROUGH) to the film surface and by placing the film sample parallel to the axis of the cylindrical camera.

The degree of orientation of a crystal plane exhibiting  $hkl$  Miller indexes  $f_{hkl}$ , with respect to the film plane, has been formalized on a quantitative numerical basis, in analogy with the Hermans' orientation functions as defined for the axial orientation in refs 20

$$f_{hkl} = (\overline{3\cos^2 \chi_{hkl}} - 1)/2 \quad (1)$$

by assuming  $\cos^2 \chi_{hkl}$  as the average cosine squared values of the angle,  $\chi_{hkl}$ , between the normal to the film surface and the normal to the  $(hkl)$  crystallographic plane.

If the direction normal to the  $hkl$  plane is unique (i.e., there are no other equivalent directions in the crystal),<sup>20</sup> a  $f_{hkl}$  is equal to +1 or -0.5 when the  $(hkl)$  crystallographic planes of all crystallites are perfectly parallel or perpendicular to the film plane, respectively. For the case of random orientation,  $f_{hkl}$  is equal to zero.

The quantity  $\cos^2 \chi_{hkl}$  has been experimentally evaluated by the above-described EDGE X-ray diffraction patterns as

$$\overline{\cos^2 \chi_{hkl}} = \overline{\cos^2 \chi_{hkl}} = \frac{\int_0^{\pi/2} I(\chi_{hkl}) \cos^2 \chi_{hkl} \sin \chi_{hkl} d\chi_{hkl}}{\int_0^{\pi/2} I(\chi_{hkl}) \sin \chi_{hkl} d\chi_{hkl}} \quad (2)$$

where  $I(\chi_{hkl})$  is the intensity distribution of a  $(hkl)$  diffraction on the Debye ring and  $\chi_{hkl}$  are the azimuthal angles measured from the horizontal lines of EDGE patterns like those of Figures 1 and 2. In particular, the diffracted intensity  $I(\chi_{hkl})$  of eq 2 has been obtained from EDGE patterns as collected by using a flat camera, by the azimuthal profile at a constant  $2\theta$  value.

Infrared spectra were obtained at a resolution of 2.0  $\text{cm}^{-1}$  with a Vector 22 Bruker spectrometer equipped with deuterated triglycine sulphate (DTGS) detector and a KBr beam splitter. The frequency scale was internally calibrated to 0.01  $\text{cm}^{-1}$  using a He–Ne laser; 32 or 16 scans were signal-averaged to reduce the noise.

**Acknowledgment.** Financial support of the “Ministero dell'Istruzione, dell'Università e della Ricerca” (PRIN2007) and of Regione Campania (Centro di Competenza) is gratefully acknowledged. Prof. Vittorio Petraccone and Dr. Oreste Tarallo of University of Naples and Prof. Vincenzo Venditto and Dr. Giuseppe Milano of University of Salerno are acknowledged for useful discussions. Dr. Dario Punzi and Claudia Rufolo are acknowledged for experimental support.

**Supporting Information Available:** X-ray diffraction patterns of the  $\gamma$  crystalline phase oriented films and quantitative comparison between observed and calculated azimuthal angles associated with  $\varepsilon$ - and  $\gamma$ -form reflections (PDF). This material is available free of charge via the Internet at <http://pubs.acs.org>.

- (18) (a) Reverchon, E.; Guerra, G.; Venditto, V. *J. Appl. Polym. Sci.* **1999**, *74*, 2077. (b) Ma, W.; Yu, J.; He, J. *Macromolecules* **2005**, *38*, 4755–4760.
- (19) Albulia, A.R.; Musto, P.; Guerra, G. *Polymer* **2006**, *47*, 234.
- (20) (a) Wilchinsky, Z. W. *Advances in X-ray Analysis*; Plenum Press: New York, 1963; Vol. 6, p 231. (b) Alexander, L. E. In *X-Ray Diffraction Methods in Polymer Science*; Krieger, R. E., Ed.; Huntington: New York, 1979; Chapter 4, p 210.